HIGHLY PRECISE PARTIAL VOLUME CORRECTION FOR PET IMAGES: AN ITERATIVE APPROACH VIA SHAPE CONSISTENCY

Ziyue Xu[1], *Ulas Bagci*[⋆,1,2], *Mingchen Gao*[1], *Daniel J. Mollura*[1]

[1]Department of Radiology and Imaging Sciences, National Institutes of Health (NIH), Bethesda, MD.
[2]Center for Research in Computer Vision (CRCV), University of Central Florida, Orlando, FL.

ABSTRACT

Positron emission tomography (PET) is capable of capturing the functional information. A major limitation for PET imaging is the low spatial resolution, leading to partial volume effects (PVE). PVE introduces significant bias to the image quantification, causing compromised measurement for uptake regions, especially smaller ones. For quantitative PET, accurate uptake values are critical for diagnostic evaluation and treatment planning. Therefore, a partial volume correction (PVC) technique is highly desirable in order to avoid size-dependent underestimation for true activities. In this paper, we present a new iterative PVC approach for PET images. The proposed method uses the state-of-the-art simultaneous delineation and noise removal algorithm to estimate the local uptake regions. The delineation is further utilized for weighted PVC with regard to a shape consistency measurement. The process is performed iteratively until delineation convergence. Qualitative and quantitative results demonstrate that the proposed framework successfully corrects the PVE and preserves local structures.

***Index Terms*—** Positron Emission Tomography, Partial Volume Correction, Shape Consistency, Regional Means, Affinity Propagation

1. INTRODUCTION

Positron emission tomography (PET) has tremendous advantages over other image modalities, such as CT and MRI, due to its ability of detecting areas of molecular biology details by accurately measuring tracer concentration in vivo. Indices characterizing tumor uptake, such as standardized uptake values (SUV), are becoming routine in PET tumor imaging. Both uptake region size and uptake value are important for accurate measurement of PET images.

However, large biases can be introduced by the partial volume effect (PVE), when tracer uptake in small tumors is measured. PVE can have a significant negative impact on the image quality too. There are basically two reasons that PVE occurs: (I) 3-D image blurring introduced by the finite spatial resolution of the imaging system, and (II) image sampling. Beside that, the biases introduced by PVE depend on numerous parameters, such as tumor size and shape, surrounding tissues and measurement method [1].

PVE can severely affect images both qualitatively and quantitatively. Such that, PVC is needed to restore the true activity distribution. Major challenges for PVC are noise and unknown uptake region definition. There is no general solution of the PVE problem, while existing algorithms fall into the following categories [2]. Some PVC methods are applied at a regional/voxel level by modifying some properties of that particular location to obtain a PVE-corrected value, such as the use of Recovery Coefficient (RC) [3], Geometric Transfer Matrix (GTM) [4], and deconvolution [5]. Another category of PVC rely on the joint use of PET images with the uptake region definitions from segmentation and/or its high resolution anatomic correspondence (CT or MRI) [6]. The goal of anatomy-based PVC methods is to utilize structural information from other imaging modalities as a prior information. Anatomical regions delineated from CT/MRI images are assumed to be functionally homogeneous. The uniformity assumption is an approximation used for the purpose of calculating the PVC.

In this paper, we presented an accurate iterative approach for PVC of PET images via shape consistency. In order to address the challenges described above, the method includes simultaneous noise removal and uptake region delineation. As shown in the flowchart for the presented scheme (Fig. 1), affinity propagation (AP) based PET image segmentation [7] is first employed to estimate the local uptake region boundaries. Then, noise is suppressed using regional means method by incorporating class information from segmentation [8]. PVE in the resulting image is further corrected with a region-based voxel-wise method [6] with the current region definition. These steps are employed iteratively to enhance the performance of each other until the convergence of AP clustering result. Since the region definition may be different during each iteration, the correction is weighted by the shape consistency between the current and previous segmen-

*Corresponding author: bagci@crcv.ucf.edu. This research is supported by CRCV of UCF, Center for Infectious Disease Imaging, the intramural research program of the National Institute of Allergy and Infectious Diseases (NIAID) and the National Institute of Biomedical Imaging and Bioengineering (NIBIB).

tations, favoring more similar delineations, or reliability in other words. In the next section, the proposed framework is presented in detail.

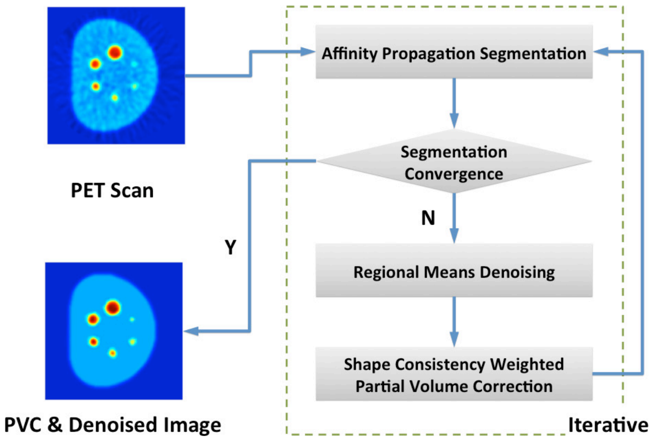

Fig. 1. Flowchart of the iterative PVC algorithm.

2. METHODS

In the presented framework, we utilized the uptake regions definition from the segmentation result to constrain the noise removal process, and to estimate the spill-over between regions. The resulting image with higher Signal-to-Noise Ratio (SNR) and higher contrast can further enhance the performance of segmentation iteratively. Therefore, robust segmentation, structure preserving denoising, and an efficient PVC algorithm are integrated.

AP based PET Image Segmentation: Robust and accurate segmentation algorithm is crucial for the proposed framework, as the denoising and PVC both relies on the estimation of uptake regions. For this purpose, we use AP algorithm [9], which has been shown to be effective for PET images in our previous studies [7, 10]. AP is an exemplar based clustering method that initially set all candidates as potential exemplars, instead of random selection that compromise global optimality. Briefly, it is utilized to identify the optimal threshold levels that separate the candidate PET images into different uptake regions. Herein, we followed our previous scheme with novel similarity functions and delineation steps as described in [7]. Also, it worths mentioning that other segmentation methods can also be applied in our PVC framework, as long as they produce accurate delineation as AP based system.

Regional Means Denoising: A major challenge for PVC is that most PVC algorithms, such as deconvolution, often lead to noise amplification. Therefore, proper denoising is needed priori to PVC. The key requirement is to enhance SNR while preserving the uptake region boundaries, so that PVC can be performed over the corrected regions, and the enhanced image can help AP to generate more precise delineations in next iterations. For this purpose, we utilized non-local means (NLM) filtering [11] for its edge preserving capability. The basic idea of NLM method is that the filtering result of a specific pixel is not only determined by its neighbors, but weighted over all pixels within the image. Practically, however, such operation is computationally too expensive, and it is often restricted within a search neighborhood. As described in [8], our proposed regional means denoising method is based on AP and NLM methods. While region information from AP clustering serves as "pre-screening" for NLM, it also covers more reliable regions over the whole image.

Shape Consistency Weighted PVC: With the region definition from AP clustering, voxel-wise PVC can be performed using the binary mask with system point spread function (PSF). To restore the true uptake value t, which is affected by PVE from a known system PSF (i.e. h), the observed image f can then be defined as: $f = t * h + n$, where $*$ is the convolution operation, and n is the noise, which is handled with regional mean denoising in the last step. The major task for PVC is to recover t from f. Here, we have designed a shape consistency based iterative method based on voxel-wise PVC scheme. First, the region definition b from AP segmentation is used to find the spill-over between voxels, and GTM method [4] is used to find the interactions between regions. Then, using the GTM corrected value g, an intermediate image is created as $s = b \cdot g$. Finally, voxel-wise correction at pixel p can be performed as

$$t(p) = f(p) \cdot \frac{s(p)}{s(p) * h}.$$

Practically, we have used an iterative scheme with shape consistency to favor later iterations when segmentation becomes stable. The shape consistency weighting parameter is evaluated with Dice Similarity Coefficient (DSC) between current and previous segmentations as $c_i = \mathrm{DSC}(b_i, b_{i+1})/N$, where N is the total iteration time and PVC is performed as

$$\begin{cases} t_0 = f, \\ t_{i+1} = t_i + c_i \cdot f \cdot \left(\frac{s_i}{s_i * h} - 1\right). \end{cases}$$

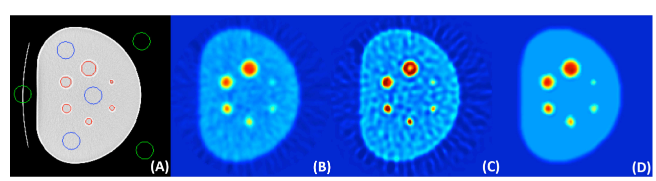

Fig. 2. PVC results: (A) the original CT image with ROI definition in high uptake regions (red), low uptake regions (blue), and background (green), (B) the original PET image, (C) result of deconvolution, (D) result of the proposed method.

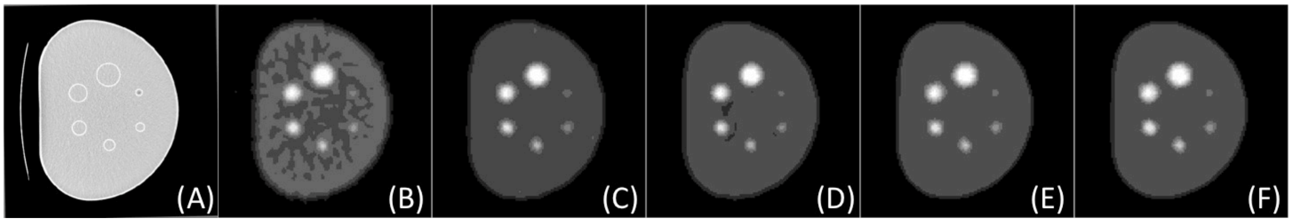

Fig. 3. Shape consistency along iterations: (A) reference CT image, (B) initial AP segmentation, (C-E) intermediate segmentation results, (F) final segmentation output at convergence.

3. EXPERIMENTS AND RESULTS

Data: In order to evaluate performance of the proposed PVC method, we used 10 PET/CT images on a NEMA phantom with different reconstruction parameters. Using phantom PET/CT images, the boundaries between each uptake region and background can be accurately defined, and the **true uptake values** are known.

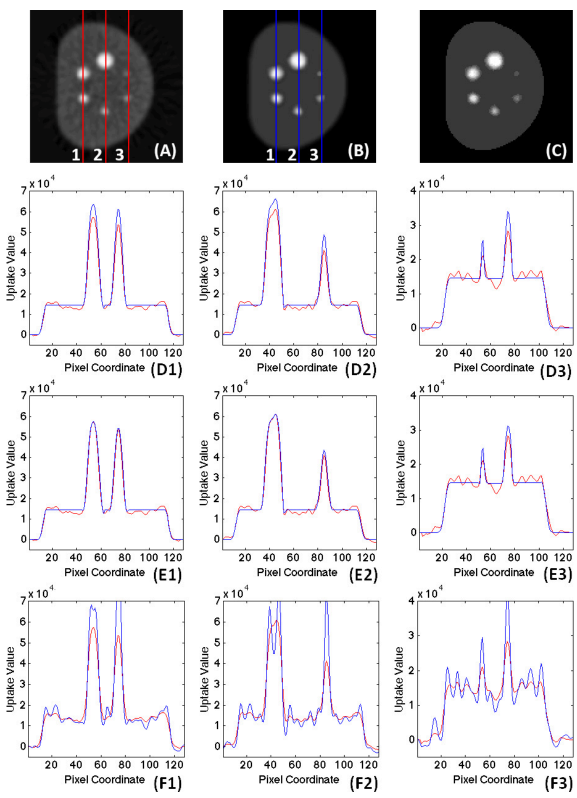

Fig. 4. Intensity profile along three (1, 2, 3) sample lines in PET image before (A) and after (B) PVE with (C) showing the final AP segmentation result: (D1-D3) the proposed method with shape consistency weights. (E1-E3) the proposed iterative method with evenly distributed weights, and (F1-F3) deconvolution method.

The phantom here contains six spheres with diameters of 10, 13, 17, 22, 28, and 37 mm, background concentration is 0.44 uCi/ml, and hot spheres concentration is 1.75 uCi/ml for all spheres. The spatial resolution is $128\times128\times47$ with spacing $2.73\times2.73\times3.27$ mm, and the image is in units of Bq/ml. The performance of the proposed iterative shape consistency weighted method is compared with deconvolution method. PVC is performed with PET image only, while the region definition for quantifications is manually traced from CT images as the ground truth.

Evaluation: As shown in Fig. 2(A), each high uptake region (red, 1-6) was accurately defined from CT scans to quantitatively evaluate the proposed algorithm. Meanwhile, ROIs in low uptake region (blue) and background (green) were randomly sampled. Statistics of PVC performance, including noise level and max uptake value, were then computed for each ROI, which were identical among original (Fig. 2(B)) and filtered images from deconvolution method (Fig. 2(C)) and the proposed method (Fig. 2(D)) for comparison. Parameter are selected according to intensity statistics from manually defined ROIs. As can be observed from the qualitative results, the proposed method successfully preserved all uptake regions, removed noise, and corrected PVE.

Here, shape consistency is evaluated between the segmentation from each iteration and the previous one. As shown in Fig. 3, AP yielded significant change at early stage of iteration (Fig. 3(B-C)), such difference became smaller and smaller along iterations (Fig. 3(C-E)) because of noise reduction and PVC performed to stabilize the appearance, and finally reached convergence (Fig. 3(F)).

To better observe the performance of the proposed method and the value of shape consistency weighting scheme, Fig. 4 illustrates intensity profiles along three sample lines (1, 2, 3 as noted in Fig. 4) within the PET image before (Fig. 4(A), red) and after (Fig. 4(B), blue) PVC. Fig. 4(C) is the final segmentation result. Fig. 4(D1-D3) shows the result given by the proposed shape consistency weighted scheme, Fig. 4(E1-E3) shows the result with even weights instead of shape consistency weights, and Fig. 4(F1-F3) illustrates the result from deconvolution. As illustrated, the proposed algorithm successfully corrects PVE for different objects and minimized the noise from the original image.

Fig. 5 presents the quantitative results of PVC as compared with phantom ground truth for object and inner background regions. Phantom ground truths are used as baseline for PVC, and the ratio is calculated to test the performance of the PVC methods, the perfect correction result in a ratio of 1. As illustrated in Fig. 5(A), the proposed method promotes the signal strength while keeping it around 1, while deconvolution result in Gibbs effect and overshooting as much as 40%. Here, the outer background is not included in the chart, because it is supposed to have a uptake value of zero, and consequently a ratio is impossible to calculate. From our experiment, the outer background ROIs have an maximum intensity (in Bq/ml) of 1676 before PVC, and 2 (proposed) and 5217 (deconvolution) after PVC. The noise reduction/amplification is shown in Fig. 5(B), noise level is calculated as the standard deviation of the intensities of the inner (low uptake region) and outer background ROIs. As shown, the proposed method successfully removed the noise from the PET image, while deconvolution greatly amplified the noise level.

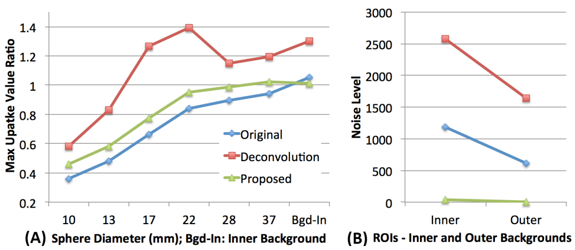

Fig. 5. Quantitative evaluations for PVC: (A) max uptake value ratio within ROIs as compared with phantom truth; (B) noise levels within background ROIs before and after PVC

4. DISCUSSION AND CONCLUSION

In this study, we presented an effective PVC method for PET images. The proposed algorithm adopts AP clustering technique for estimating different level of uptake regions, and this information is further incorporated within a regional means denoising algorithm and PVC method to enhance the image. The process is designed in an iterative manner, and PVC is performed with shape consistency weighting, which in turn helps promoting the accuracy of segmentation. Experimental results demonstrated that the proposed framework is effective in preserving small uptake regions and effectively corrects the PVE from PET images. Note that for small and low contrast lesions, the current framework employs a conservative strategy to avoid potential over-correction and false-positives, a future work would be to correctly identify true small lesions and perform PVC without over estimation.

5. REFERENCES

[1] M. Soret, S. L. Bacharach, and I. Buvat, "Partial-volume effect in PET tumor imaging," *Journal of Nuclear Medicine*, vol. 48, no. 6, pp. 932–945, 2007.

[2] K. Erlandsson, I. Buvat, P. H. Pretorius, B. A. Thomas, and B. F. Hutton, "A review of partial volume correction techniques for emission tomography and their applications in neurology, cardiology and oncology," *Physics in Medicine and Biology*, vol. 57, no. 21, pp. R119, 2012.

[3] F. Gallivanone, A. Stefano, E. Grosso, C. Canevari, L. Gianolli, C. Messa, M.-C. Gilardi, and I. Castiglioni, "PVE correction in PET-CT whole-body oncological studies from PVE-affected images," *IEEE Trans. on Nuclear Science*, vol. 58, no. 3, pp. 736–747, June 2011.

[4] O. G. Rousset, Y. Ma, and A. C. Evans, "Correction for partial volume effects in PET: Principle and validation," *Journal of Nuclear Medicine*, vol. 39, no. 5, pp. 904–911, 1998.

[5] J. Tohka and A. Reilhac, "Deconvolution-based partial volume correction in Raclopride-PET and Monte Carlo comparison to MR-based method," *NeuroImage*, vol. 39, no. 4, pp. 1570 – 1584, 2008.

[6] B. A. Thomas, K. Erlandsson, M. Modat, L. Thurfjell, R. Vandenberghe, S. Ourselin, and B. F. Hutton, "The importance of appropriate partial volume correction for PET quantification in Alzheimer's disease," *European Journal of Nuclear Medicine and Molecular Imaging*, vol. 38, no. 6, pp. 1104–1119, 2011.

[7] B. Foster, U. Bagci, Z. Xu, B. Dey, B. Luna, W. Bishai, S. Jain, and D. J. Mollura, "Segmentation of PET images for computer-aided functional quantification of tuberculosis in small animal models," *IEEE Trans. on Biomedical Engineering*, vol. 61, no. 3, pp. 711–724, March 2014.

[8] Z. Xu, U. Bagci, J. Seidel, D. Thomasson, J. Solomon, and D. J. Mollura, "Segmentation based denoising of PET images: An iterative approach via regional means and affinity propagation," in *Medical Image Computing and Computer-Assisted Intervention, MICCAI 2014*, vol. 8673 of *Lecture Notes in Computer Science*, pp. 698–705. Springer International Publishing, 2014.

[9] B. J. Frey and D. Dueck, "Clustering by passing messages between data points," *Science*, vol. 315, no. 5814, pp. 972–976, 2007.

[10] B. Foster, U. Bagci, B. Luna, B. Dey, W. Bishai, S. Jain, Z. Xu, and D. J. Mollura, "Robust segmentation and accurate target definition for positron emission tomography images using affinity propagation," in *IEEE 10th International Symposium on Biomedical Imaging (ISBI), 2013*, April 2013, pp. 1461–1464.

[11] A. Buades, B. Coll, and J.-M. Morel, "A non-local algorithm for image denoising," in *IEEE Computer Society Conference on Computer Vision and Pattern Recognition, CVPR 2005*, June 2005, vol. 2, pp. 60–65.